International Journal of Heat and Technology
Vol. 44, No. 2, April, 2026, pp. 861-872
Journal homepage: http://iieta.org/journals/ijht

Temperature-Dependent Gibbs Free Energy of Low-Concentration Nitrogen and Phosphorus Removal by Ceramsite Reverse Filter Layers: Insights from Isothermal Adsorption Thermodynamics

Bo Zhou[1], Jiangqi Wu[1], Jintao Shi[1], Feng Zhang[2], Shuyao Ma[1], Xuan Wang[1*]

[1] College of Electrical and Control Engineering, Ningxia Polytechnic University of Business and Technology, Yinchuan 750021, China
[2] Ningxia Yuanyi Spatial Information Technology Co., Ltd, Yinchuan 750021, China

Corresponding Author Email: zbzb.8160@163.com

https://doi.org/10.18280/ijht.440236

Received: 26 October 2025
Revised: 23 February 2026
Accepted: 18 March 2026
Available online: 30 April 2026

Keywords:
ceramsite reverse filter layer, low-concentration nitrogen and phosphorus, isothermal adsorption thermodynamics, Gibbs free energy, temperature dependence, heat capacity effect, selective thermodynamics

ABSTRACT

Eutrophication driven by low-concentration nitrogen and phosphorus has become a global environmental challenge. Ceramsite reverse filter layers, characterized by their porous structure, high stability, and low cost, have demonstrated considerable potential for mitigating such pollution. Temperature, as a critical environmental factor governing solid–liquid interfacial adsorption, primarily regulates thermodynamic behavior through its effect on Gibbs free energy. However, existing studies often suffer from oversimplified equilibrium constant calculations, inappropriate assumptions of constant enthalpy and entropy, disconnection between equilibrium and dynamic processes, and inadequate interpretation of selective thermodynamics in multi-component systems. To address these limitations, this study integrates static and dynamic adsorption experiments with innovative approaches including non-ideal activity correction, heat capacity effect incorporation, transition state thermodynamics coupling, and selective Gibbs free energy quantification. The temperature-dependent regulatory mechanisms of Gibbs free energy in the adsorption of low-concentration nitrogen and phosphorus by ceramsite reverse filter layers were systematically investigated. A rigorous method for calculating true thermodynamic equilibrium constants under non-ideal conditions was established, overcoming conventional concentration-based simplifications. Heat capacity effects were introduced to correct the temperature dependence of Gibbs free energy, revealing the dynamic evolution of enthalpy and entropy with temperature. The coupling of static equilibrium thermodynamics and dynamic transition state thermodynamics was achieved, linking equilibrium parameters with activation parameters. Furthermore, a selective Gibbs free energy evaluation method for competitive ions was proposed, enhancing the thermodynamic framework for multi-component systems. The results indicate that temperature significantly influences the energy distribution of adsorption sites on ceramsite surfaces, the spontaneity of adsorption, and the activation energy barrier. The developed temperature-dependent thermodynamic equation enables accurate prediction of the adsorption performance of reverse filter layers. This study provides strict thermodynamic criteria for the engineering optimization of ceramsite reverse filters in low-concentration nitrogen and phosphorus pollution control, enriches the theoretical system of solid–liquid interface adsorption thermodynamics, and offers a transferable paradigm for thermodynamic research on analogous environmental functional materials.

1. INTRODUCTION

Low-concentration nitrogen and phosphorus pollution [1, 2] is widespread in agricultural non-point source emissions, treated wastewater effluents, and natural water bodies. The resulting eutrophication not only disrupts the balance of aquatic ecosystems but also threatens drinking water safety, making it a key challenge and difficulty in the field of global environmental governance. Current technologies for treating low-concentration nitrogen and phosphorus [3, 4] face bottlenecks such as insufficient adsorption spontaneity and poor reaction reversibility. The essence of these issues lies in the unclear thermodynamic regulation mechanisms, failing to fundamentally reveal the influence laws of key environmental factors such as temperature on the adsorption process. As a novel environmental functional material, ceramsite reverse filter layers [5, 6] demonstrate unique application potential in the adsorption and removal of low-concentration pollutants due to their high specific surface area derived from porous structures, excellent chemical stability, and low-cost advantages. The temperature dependence of adsorption performance is a core consideration for the engineering

application of ceramsite reverse filter layers. The essence of this dependence is the regulation of thermodynamic parameters by temperature, among which Gibbs free energy [7, 8], as the core criterion for judging the spontaneity of the adsorption process, is the key to revealing the temperature regulation mechanism and optimizing engineering operating conditions. The current research orientation of thermodynamics journals focuses on the precise calculation of solid-liquid interface thermodynamic parameters [9, 10], thermodynamic corrections for non-ideal systems, and the deep integration of theory and engineering applications. This study precisely meets this demand for disciplinary development, combining theoretical innovation with engineering application value.

Although research on the adsorption of low-concentration nitrogen and phosphorus by ceramsite has made some progress, existing thermodynamic studies still suffer from many limitations, which severely restrict the improvement of theoretical depth and engineering application value. Traditional adsorption thermodynamics [11, 12] studies generally use concentration instead of activity to calculate equilibrium constants, ignoring the non-ideal behavior of low-concentration ions. This leads to systematic deviations in Gibbs free energy calculations and lacks thermodynamic rigor. At the same time, most studies assume that the standard enthalpy change and standard entropy change do not vary with temperature, ignoring the heat capacity effect [13, 14] brought about by solvent reorganization and surface desolvation during the solid-liquid adsorption process, thus failing to accurately describe the temperature-dependent characteristics of Gibbs free energy [15, 16]. There is a significant disconnect between static adsorption thermodynamics and dynamic engineering applications. Existing studies have not effectively coupled the equilibrium-state Gibbs free energy with the activation thermodynamic parameters of the dynamic breakthrough process, making it difficult to support the temperature regulation needs in practical engineering. In multi-component complex water bodies, research on adsorption selectivity [17, 18] under competing coexisting ions mostly remains at the level of adsorption capacity, lacking explanations of the thermodynamic essence and failing to reveal the regulation mechanism of temperature on adsorption selectivity. Furthermore, existing studies have not yet constructed a unified temperature-dependent thermodynamic equation of state [19, 20], making it difficult to achieve accurate predictions of the adsorption performance of reverse filter layers under different environmental conditions; thus, the theoretical system still requires improvement.

In response to the aforementioned research gaps, this study conducts a systematic investigation focusing on the regulation mechanism of temperature on the Gibbs free energy of low-concentration nitrogen and phosphorus adsorption by ceramsite reverse filter layers, proposing a series of innovative thermodynamic research methods and theoretical systems. The extended Debye-Hückel equation is used to calculate solution-phase activity coefficients, combined with the Frumkin-Fowler-Guggenheim model to correct adsorption phase activity, accurately obtaining the true thermodynamic equilibrium constant and unbiased standard Gibbs free energy, effectively solving the problem of systematic errors in traditional calculations. Through the fitting of multi-temperature static experimental data, a temperature-dependent Gibbs free energy model incorporating the heat capacity effect is established, deriving temperature-dependent enthalpy change and entropy change functions, revealing the microscopic mechanism of Gibbs free energy variation with temperature, and significantly improving the accuracy of thermodynamic parameter calculations. Combining dynamic column experiments, the Yoon-Nelson model, and the Eyring equation, the coupling of static equilibrium thermodynamics and dynamic transition state thermodynamics is realized, clarifying the thermodynamic regulation mechanism of temperature on adsorption rate, and establishing thermodynamic criteria for temperature-flow rate-removal efficiency. Based on the multi-component Langmuir model, ion exchange equilibrium constants are derived, selective Gibbs free energy is defined, and a competitive ion selective thermodynamics evaluation system is constructed, providing theoretical support for applications in complex water bodies. Finally, all thermodynamic parameters are integrated to establish a temperature-dependent thermodynamic equation of state for the removal of low-concentration nitrogen and phosphorus by ceramsite reverse filter layers, filling the gap in existing research and realizing the deep integration of theoretical research and engineering applications.

2. PROPOSED METHODS

2.1 Core research framework

This study takes the regulation mechanism of temperature on the Gibbs free energy of low-concentration nitrogen and phosphorus adsorption by ceramsite reverse filter layers as the core research thread. Following the systematic research logic of material characterization, static adsorption experiments, dynamic filtration experiments, thermodynamic parameter correction, coupling of equilibrium and activation parameters, and finally the construction of a thermodynamic equation of state, this study realizes a full-chain research from thermodynamic correction of non-ideal systems to the construction of an engineering-oriented equation of state. The entire process highlights the deep integration of adsorption thermodynamics theoretical innovation and the engineering application of low-concentration nitrogen and phosphorus pollution control, ensuring that the research results possess both thermodynamic rigor and engineering practicality. It provides a clear and systematic research framework for subsequent thermodynamic parameter analysis, temperature regulation mechanism revelation, and engineering optimization.

2.2 Thermodynamic characterization of ceramsite reverse filter layer materials

Industrial waste residue and a pore-forming agent were mixed uniformly at a mass ratio of 7 : 3, and the ceramsite substrate was prepared via high-temperature sintering at 1050 ℃. Subsequently, modification treatment was carried out by immersion in a 0.5 mol/L $FeCl_3$ solution to introduce α-FeOOH and α-Fe_2O_3 active components onto the ceramsite surface. The samples were dried at 60 ℃ before use. This modification process can significantly increase the number of active sites and reactivity on the ceramsite surface, optimize the surface charge distribution and interface thermodynamic properties, and provide an adsorption carrier with excellent structure and performance for the subsequent thermodynamic study of low-concentration nitrogen and phosphorus

adsorption, ensuring the precise determination of thermodynamic parameters and the reliability of mechanism analysis for the adsorption process.

The core thermodynamic characterization of the ceramsite reverse filter layer focuses on the precise acquisition of adsorption-related basic parameters, providing support for Gibbs free energy calculation and regulation mechanism analysis. The potentiometric titration method was used to determine the site density and surface acid-base equilibrium constants of the ceramsite, and the isoelectric point was obtained combined with Zeta potential analysis. These parameters are directly used to analyze the energy distribution characteristics of adsorption sites, providing basic data support for the precise calculation of Gibbs free energy. Meanwhile, a microcalorimetric isothermal titration calorimeter was used to measure the thermal effects of the nitrogen and phosphorus adsorption process at 298 K. This parameter verifies the consistency of the adsorption thermodynamic pathway and the reaction reversibility, further guaranteeing the reliability of the subsequent Gibbs free energy calculation results, and laying a solid experimental foundation for the entire thermodynamic research system.

2.3 Non-ideal activity correction and real Gibbs free energy calculation

In low-concentration nitrogen and phosphorus adsorption systems, the ionic strength is relatively low. Traditional adsorption thermodynamics studies often use concentration directly instead of activity to calculate the equilibrium constant, ignoring the non-ideal behavior of low-concentration ions, which leads to systematic deviations in Gibbs free energy calculations. To address this issue, this study targets dilute solution systems with an ionic strength of 0.01 mol·L^{-1} and uses the extended Debye-Hückel equation to calculate the single-ion activity coefficient γ_i. Its expression is:

$$\log_{10}\gamma_i = -\frac{Az_i^2\sqrt{I}}{1+Ba_i\sqrt{I}} + bI \quad (1)$$

where, A and B are temperature-dependent Debye constants, z_i is the ion charge number, a_i is the ionic radius parameter, and b is set to 0.1 to adapt to the non-ideality correction of low ionic strength systems. Based on the calculated single-ion activity coefficients, the activity a_i of nitrogen and phosphorus species in the solution can be determined by $a_i=\gamma_i C_i$, where C_i is the equilibrium concentration of nitrogen and phosphorus ions. This correction method can accurately quantify the non-ideal effects brought by interionic interactions in low-concentration systems, providing a reliable basis for the subsequent calculation of real equilibrium const/ants.

The non-ideal characteristics of the adsorption phase also affect the accuracy of the thermodynamic equilibrium constant. Traditional studies mostly assume that the adsorption phase is an ideal system, ignoring the interaction between adsorption sites, leading to deviations in the calculation of adsorption phase activity. This study uses the Frumkin-Fowler-Guggenheim model to correct the adsorption phase activity. First, the fractional occupation of adsorption sites θ is calculated through adsorption isotherm data, which is defined as the ratio of the equilibrium adsorption amount q_e to the saturated adsorption amount q_m, namely $\theta = q_e/q_m$. On this basis, combined with the lateral interaction parameter ω between adsorption sites, the calculation formula for the adsorption phase surface activity $a_{s,i}$ is obtained as $a_{s,i} = \theta_i exp(\omega\theta_i)$, where the value of ω is determined by fitting the adsorption isotherm and is used to characterize the attractive or repulsive interaction between adsorption sites. This correction can effectively reflect the non-ideality of the adsorption phase and improve the accuracy of adsorption phase activity calculation. Figure 1 shows the flowchart of dual-phase activity correction and real standard Gibbs free energy calculation for non-ideal solid-liquid systems.

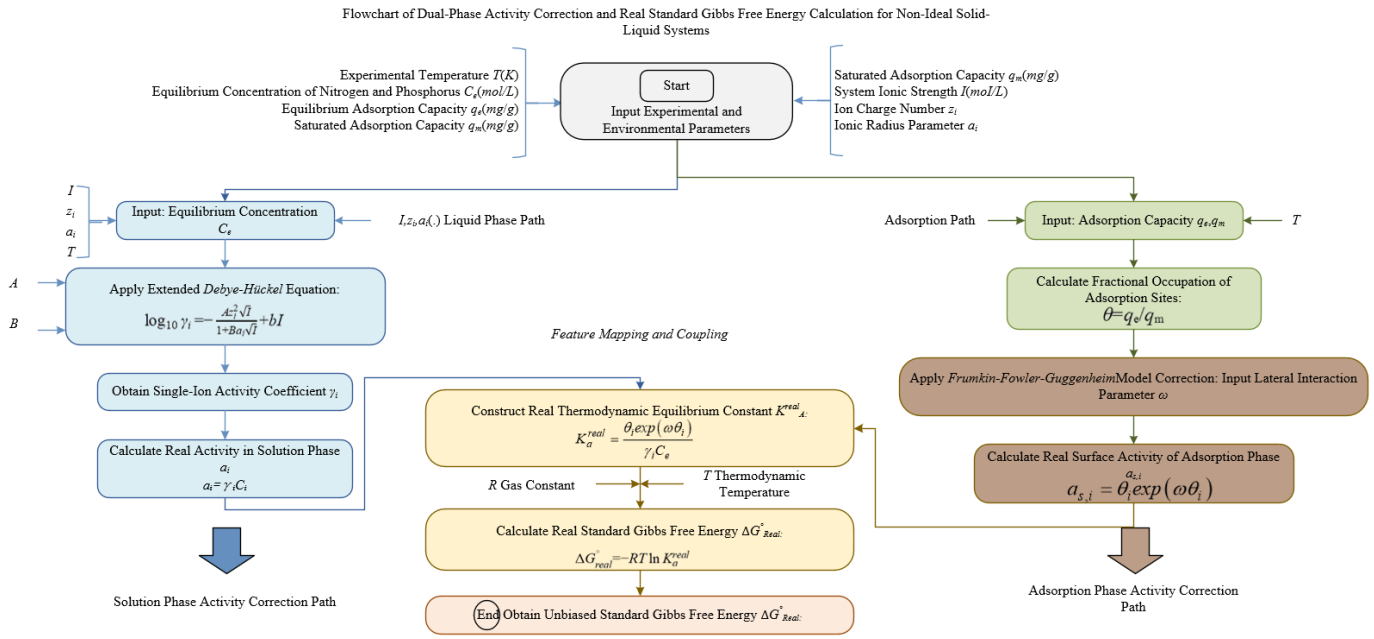

Figure 1. Flowchart of dual-phase activity correction and real standard Gibbs free energy calculation for non-ideal solid-liquid systems

Based on the dual activity correction of the solution phase and the adsorption phase, a calculation method for the real thermodynamic equilibrium constant K_a^{real} is constructed, and its expression is:

$$K_a^{real}=\frac{\theta_i exp(\omega\theta_i)}{\gamma_i C_e} \quad (2)$$

Combining the basic thermodynamic relations, the real standard Gibbs free energy is calculated by the following formula:

$$\Delta G^{\circ}_{real}=-RT\ln K_a^{real} \quad (3)$$

where, R is the gas constant and T is the thermodynamic temperature. This calculation process integrates the effects of solution-phase ionic non-ideality and adsorption phase site interactions, effectively breaking away from the limitations of traditional concentration simplification assumptions. It can obtain an unbiased real standard Gibbs free energy, significantly improving the rigor of adsorption thermodynamics calculations, and providing accurate basic parameters for subsequent temperature dependence analysis and thermodynamic regulation mechanism revelation.

2.4 Gibbs free energy temperature dependence model incorporating heat capacity effect

During the solid-liquid interface adsorption process, solvent reorganization, surface desolvation, and ion coordination will induce heat capacity changes. Traditional Gibbs free energy temperature dependence models generally assume that the constant pressure heat capacity is zero, ignoring the impact of the aforementioned heat capacity effects, leading to deviations in the description of how Gibbs free energy changes with temperature, and failing to accurately reflect the temperature regulation mechanism. To solve this problem, this study introduces constant pressure heat capacity into the model construction, breaking through the limitations of traditional assumptions, and expands the standard Gibbs free energy into a nonlinear function containing constant pressure heat capacity. Its expression is:

$$\Delta G^{\circ}(T)=\Delta H^{\circ}(T_0)-T\Delta S^{\circ}(T_0)+\Delta C_p\left[(T-T_0)-T\ln\left(\frac{T}{T_0}\right)\right] \quad (4)$$

where, T_0 is taken as 298.15 K as the reference temperature, $H^{\circ}(T_0)$ and $\Delta S^{\circ}(T_0)$ are the standard enthalpy change and standard entropy change at the reference temperature respectively, and ΔC_p is the constant pressure heat capacity of the adsorption process. By introducing the heat capacity effect term, this model can accurately quantify the influence of enthalpy-entropy coupling on Gibbs free energy during temperature changes, improving the description of temperature dependence characteristics.

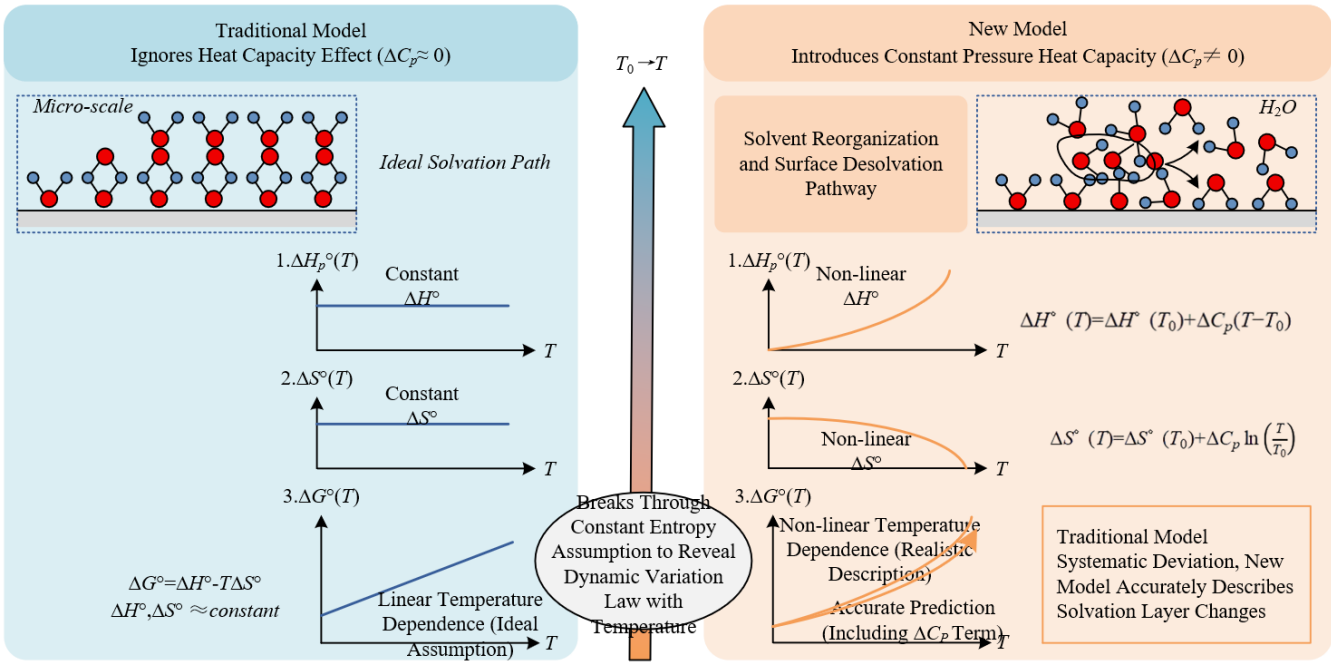

Figure 2. Comparison and evolution diagram of the Gibbs free energy temperature dependence model incorporating constant pressure heat capacity and the traditional model

Figure 2 shows the comparison and evolution diagram of the Gibbs free energy temperature dependence model incorporating constant pressure heat capacity and the traditional model. Accurate fitting of model parameters is the key to ensuring the accuracy of Gibbs free energy calculation and prediction. This study uses the real standard Gibbs free energy data obtained from multi-temperature static adsorption experiments for parameter fitting. Five temperature points were set for the experiments: 278 K, 288 K, 298 K, 308 K, and 318 K. This temperature range covers the common ambient temperature interval of natural water bodies, ensuring the practical application value of the fitting results. Based on the ΔG°_{real} data corresponding to the above temperature points, the least squares method was used to simultaneously fit the three core parameters: $\Delta H^{\circ}(T_0)$, $\Delta S^{\circ}(T_0)$, and ΔC_p. During the fitting process, ΔC_p is assumed to be constant within the narrow temperature range. This assumption not only conforms to the thermodynamic characteristics of the solid-liquid adsorption system but also simplifies the fitting process while ensuring the reliability and accuracy of the parameters, laying the foundation for the subsequent derivation of temperature-dependent enthalpy and entropy functions.

Based on the fitted parameter ΔC_p, the temperature-dependent standard enthalpy change and standard entropy

change functions are further derived to improve the temperature response mechanism of Gibbs free energy. According to the basic thermodynamic relations, the variation of standard enthalpy change with temperature can be described by the following formula:

$$\Delta H^{\circ}(T)=\Delta H^{\circ}(T_0)+\Delta C_p(T-T_0) \tag{5}$$

Correspondingly, the temperature dependence function of standard entropy change is:

$$\Delta S^{\circ}(T)=\Delta S^{\circ}(T_0)+\Delta C_p \ln\left(\frac{T}{T_0}\right) \tag{6}$$

The above two functions clearly reveal the regulatory effect of ΔC_p on enthalpy and entropy parameters, clarify the dynamic change law of enthalpy and entropy with temperature, and break the limitation of constant enthalpy and entropy in traditional models. By substituting the temperature-dependent enthalpy and entropy functions into the Gibbs free energy model, the accurate calculation and prediction of $\Delta G^{\circ}(T)$ at different temperatures can be realized, significantly improving the prediction accuracy of thermodynamic parameters, and providing reliable theoretical support for the subsequent analysis of the temperature regulation mechanism on adsorption spontaneity.

2.5 Coupling of dynamic transition state thermodynamics and equilibrium state Gibbs free energy

Figure 3 gives a schematic diagram showing the coupling mechanism between static equilibrium thermodynamics and dynamic transition state kinetics. Static adsorption thermodynamics can only characterize the characteristics of the system equilibrium state and is difficult to reflect the mass transfer and reaction laws of the actual dynamic operation process of the ceramsite reverse filter layer. To establish the intrinsic connection between the dynamic process and thermodynamic parameters, this study uses the Yoon-Nelson model to quantitatively fit the column experiment breakthrough curves under different temperature conditions. The model expression is written as:

$$\frac{C_t}{C_0}=\frac{1}{1+exp[k_{YN}(t-\tau)]} \tag{7}$$

where, C_t and C_0 represent the effluent and influent pollutant concentrations of the column device respectively, k_{YN} characterizes the apparent rate constant of the adsorption process, and τ corresponds to the characteristic time when the pollutant penetration ratio reaches 50%. The kinetic characteristic parameters at different temperatures can be accurately extracted through fitting, providing reliable experimental data support for the subsequent quantitative solution of transition state thermodynamic parameters.

Based on the transition state theory framework, the apparent rate constant obtained from breakthrough curve fitting is correlated with temperature, and the Eyring equation is used to transform kinetic parameters into activated thermodynamic parameters. After linear transformation, the following expression is obtained:

$$\ln\left(\frac{k_{YN}}{T}\right)=-\frac{\Delta H^{\ddagger}}{R}\cdot\frac{1}{T}+\ln\left(\frac{k_B}{h}\right)+\frac{\Delta S^{\ddagger}}{R} \tag{8}$$

where, k_B is the Boltzmann constant, h is the Planck constant, and $\Delta H^{\ddagger}$ and $\Delta S^{\ddagger}$ are the activation enthalpy and activation entropy of the adsorption process, respectively. Using the fitting data under multi-temperature working conditions for linear regression, the activation enthalpy and activation entropy can be solved, and then the activation Gibbs free energy $\Delta G^{\ddagger}$ can be calculated based on the basic thermodynamic relationship, realizing the thermodynamic quantitative characterization of the microscopic energy barrier characteristics of the dynamic adsorption process.

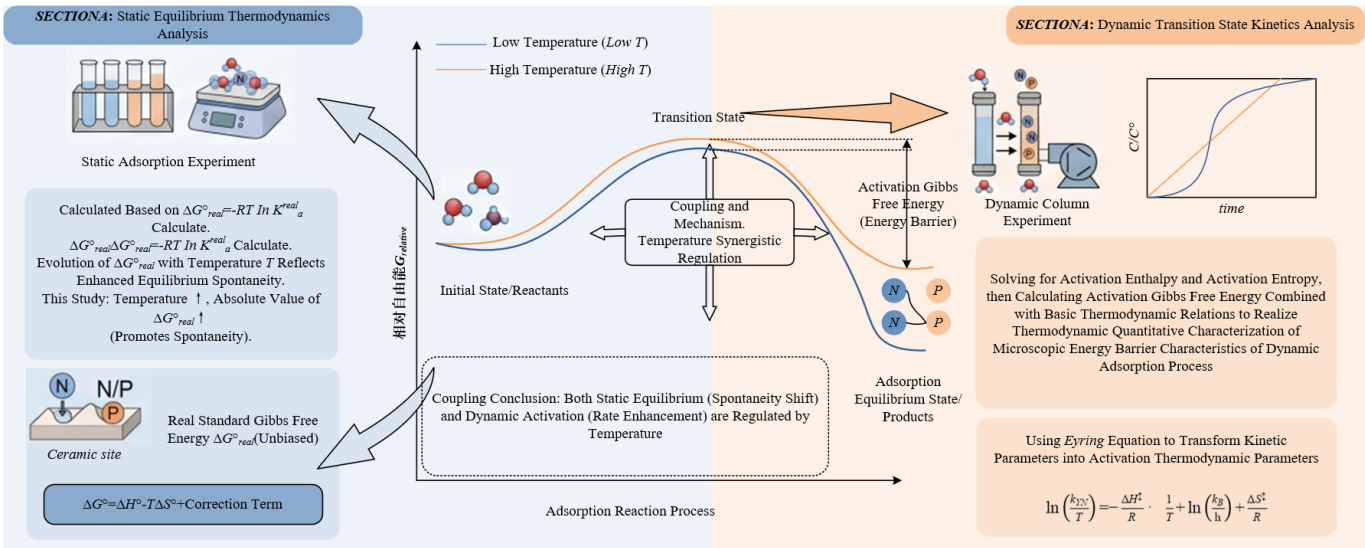

Figure 3. Schematic diagram of the coupling mechanism between static equilibrium thermodynamics and dynamic transition state kinetics

Existing studies mostly conduct separate analyses of equilibrium thermodynamics or dynamic kinetics, lacking the intrinsic correlation analysis of the two types of parameters. This study performs a synergistic comparison between the equilibrium-state Gibbs free energy corrected by the non-ideal system ΔG°_{real} and the transition-state activation Gibbs free

energy $\Delta G^{\ddagger}$. Based on the evolution law of the two types of parameters with temperature, the main controlling mechanism of the adsorption process is identified, effectively distinguishing between intraparticle diffusion control and surface chemical reaction control modes. Relying on the coupling relationship between equilibrium parameters and activation parameters, the synergistic regulation law of temperature on adsorption equilibrium spontaneity and dynamic reaction energy barriers can be analyzed, and then the thermodynamic correlation basis among temperature, operating flow rate, and pollutant removal efficiency is established, providing theoretical support for the temperature optimization and operating parameter regulation of ceramsite reverse filter layer engineering conditions.

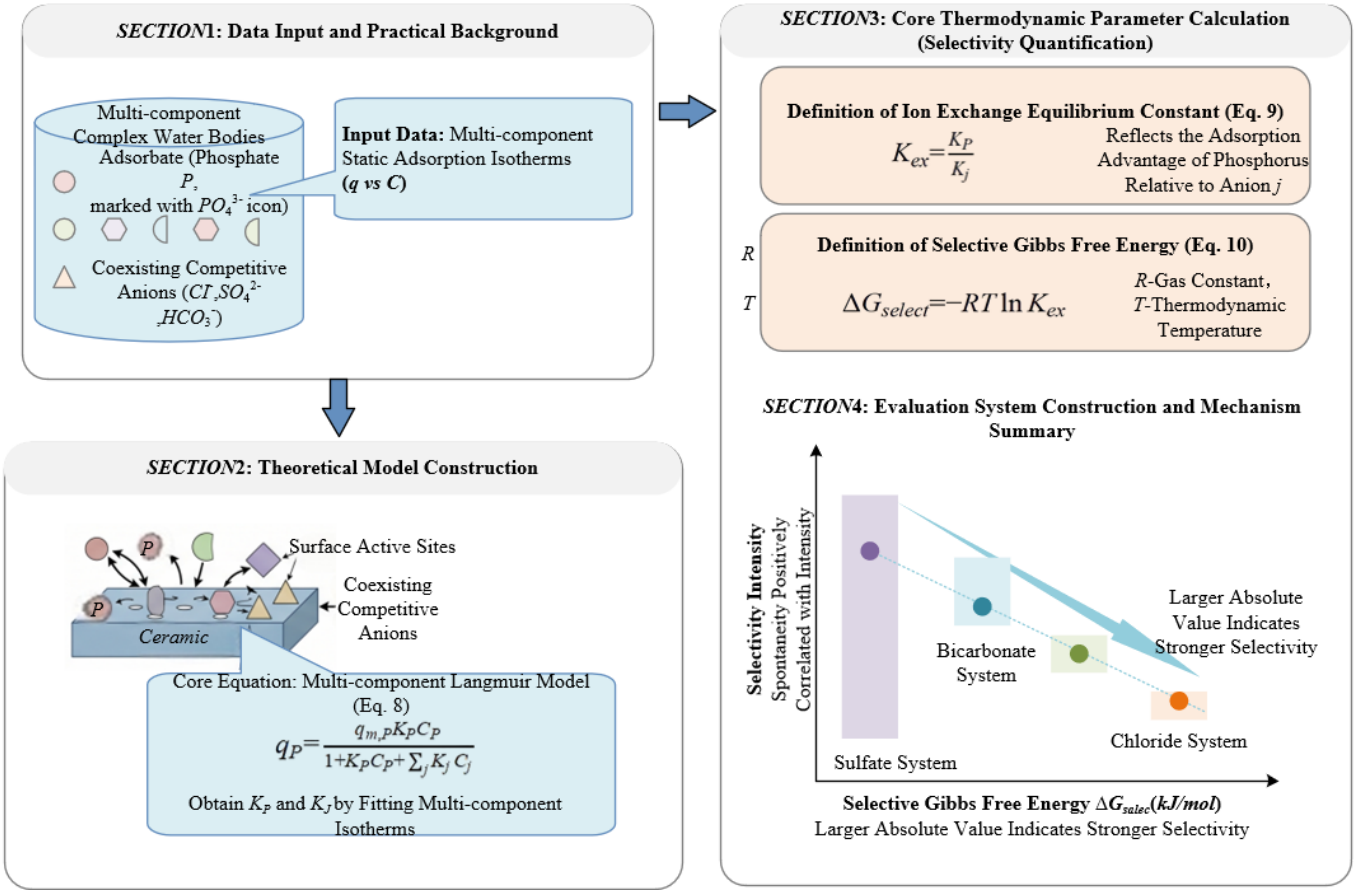

Figure 4. Construction mechanism diagram of selective thermodynamics evaluation system for coexisting anion competitive adsorption in multi-component complex water bodies

2.6 Calculation of competitive ion selective Gibbs free energy

Natural water bodies and treated wastewater effluents often contain coexisting anions such as chloride, sulfate, and bicarbonate. These ions compete with phosphorus for adsorption, affecting the adsorption performance of ceramsite reverse filter layers. To quantify the thermodynamic essence of this competition effect, this study uses the multi-component Langmuir model to fit the adsorption isotherms in the presence of coexisting ions, analyzing the selective adsorption characteristics of ceramsite for phosphorus through model parameters. The model expression is:

$$q_P=\frac{q_{m,P}K_PC_P}{1+K_PC_P+\sum_j K_j C_j} \tag{9}$$

where, q_P is the equilibrium adsorption amount of phosphorus by ceramsite, $q_{m,P}$ is the saturated adsorption amount of phosphorus by ceramsite, K_P is the adsorption equilibrium constant of phosphorus, K_j is the adsorption equilibrium constant of various coexisting anions, and C_P and C_j are the equilibrium concentrations of phosphorus K_P and coexisting anions K_j, respectively. The and of different coexisting anions can be accurately obtained through isotherm data fitting, providing core parameter support for the subsequent thermodynamic quantitative analysis of selectivity. Figure 4 shows the construction mechanism diagram of the selective thermodynamics evaluation system for coexisting anion competitive adsorption in multi-component complex water bodies.

Based on the fitted adsorption equilibrium constants, the ion exchange equilibrium constant K_{ex} between phosphorus and coexisting anions is defined, and its calculation formula is:

$$K_{ex}=\frac{K_P}{K_j} \tag{10}$$

This constant can directly reflect the relative adsorption selectivity of ceramsite for phosphorus compared to coexisting anions. Combining the basic thermodynamic relations, the selective Gibbs free energy ΔG_{select} is further derived, and its expression is:

$$\Delta G_{select}=-RT\ln K_{ex} \tag{11}$$

where, R is the gas constant and T is the thermodynamic temperature. Through this calculation method, the selectivity of ceramsite for phosphorus can be quantified from the thermodynamic essence. By analyzing the variation law of at different temperatures ΔG_{select}, the regulation mechanism of temperature on adsorption selectivity can be clarified. At the same time, it avoids the limitation of traditional research that only describes selectivity from the perspective of adsorption capacity, providing accurate thermodynamic theoretical support for the application of ceramsite reverse filter layers in complex multi-component water bodies.

2.7 Construction of temperature-dependent thermodynamic equation of state

This study integrates the complete set of thermodynamic characteristic parameters obtained above, including real standard Gibbs free energy, temperature-dependent enthalpy and entropy functions, constant pressure heat capacity, activation thermodynamic parameters, and selective Gibbs free energy. Based on the law of mass action as the fundamental framework, combined with the modified form of the Van't Hoff relation, the equation derivation is carried out to couple the microscopic thermodynamic laws of the solid-liquid interface with macro-environmental working condition factors. By normalizing the adsorption equilibrium relative concentration as the state response quantity, a multi-variable coupled thermodynamic equation of state is constructed:

$$\frac{C_{eq}}{C_0}=f(T,pH,I,\text{Flow Rate, Type of Competing Ions}) \quad (12)$$

This equation incorporates thermodynamic temperature, system acid-base conditions, ionic strength, reverse filter layer operating flow rate, and coexisting competing ion types into a unified variable system, breaking away from the limitation of traditional research that could only fit adsorption behavior under single conditions. Relying on the intrinsic constraint relationship of complete thermodynamic parameters, the synergistic influence of various environmental and operating factors on the equilibrium residual concentration of nitrogen and phosphorus can be quantitatively characterized. It realizes the quantitative prediction of the adsorption equilibrium efficiency and dynamic breakthrough characteristics of ceramsite reverse filter layers under different water quality conditions and operating conditions, establishes a direct link between adsorption thermodynamics theory and actual filter layer engineering regulation, and further improves the thermodynamic theoretical system of low-concentration nitrogen and phosphorus solid-liquid adsorption systems.

3. EXPERIMENTAL SECTION

3.1 Experimental materials and instruments

The raw materials used in this study were fly ash and shale industrial waste residue, combined with a pore-forming agent to prepare the ceramsite substrate. The modification reagent used was ferric chloride hexahydrate. Ammonium chloride and potassium dihydrogen phosphate were selected as adsorbates to prepare low-concentration nitrogen and phosphorus simulated wastewater. Coexisting competitive ions were provided by sodium chloride, sodium sulfate, and sodium bicarbonate. All chemical reagents were of analytical grade. Deionized water with a conductivity lower than 10 μS/cm was used throughout the experiment to prepare solutions, avoiding interference from background ions in the water body on the non-ideal thermodynamic behavior of the low-concentration system.

Table 1. Basic information of main experimental reagents

Reagent Name	Chemical Formula	Purity Grade	Specification
Ferric chloride hexahydrate	$FeCl_3 \cdot 6H_2O$	Analytical pure	500 *g*
Ammonium chloride	NH_4Cl	Analytical pure	500 *g*
Potassium dihydrogen phosphate	KH_2PO_4	Analytical pure	500 *g*
Sodium chloride	$NaCl$	Analytical pure	500 *g*
Sodium sulfate	Na_2SO_4	Analytical pure	500 *g*
Sodium bicarbonate	$NaHCO_3$	Analytical pure	500 *g*

Table 2. Core experimental instruments and technical parameters

Instrument Name	Key Technical Indicators	Application Description
High-temperature sintering furnace	Temperature control accuracy ±5 ℃	Preparation of ceramsite by high-temperature sintering
Automatic potentiometric titrator	pH test accuracy ±0.01	Determination of surface site density and acid-base constants
Zeta potential analyzer	Potential test accuracy ±0.1 mV	Characterization of ceramsite surface isoelectric point
Microcalorimetric isothermal titration calorimeter	Heat effect detection accuracy ±0.1 μJ	Determination of microcalorimetric effects of adsorption process
Constant temperature water bath shaker	Temperature control accuracy ±0.1 K	Multi-temperature static adsorption equilibrium experiments
Upflow fixed-bed adsorption column device	Column inner diameter 2.5 cm, controllable constant flow rate	Dynamic reverse filter layer breakthrough experiments
High performance liquid chromatograph	Concentration detection limit 0.01 $mg \cdot L^{-1}$	Quantitative detection of nitrogen and phosphorus equilibrium concentrations
Electronic analytical balance	Weighing accuracy 0.0001 g	Accurate weighing of reagents and samples

The equipment selected for the experiment meets the requirements for precise thermodynamic characterization and quantitative testing, covering instruments for the entire process including high-temperature material preparation, surface physicochemical characterization, microcalorimetry measurement, constant temperature adsorption, dynamic

column reactions, and concentration detection. The temperature control and detection accuracy of each instrument ensure the reliability of thermodynamic parameter fitting and calculation.

As shown in Tables 1 and 2, the purity of the experimental reagents can eliminate the interference of impurity ions on the low-concentration adsorption system. The high-precision indicators for temperature control, microcalorimetry, and concentration detection are suitable for refined thermodynamic research needs such as non-ideal activity correction, heat capacity effect fitting, and transition state thermodynamic parameter solving, ensuring the credibility of subsequent experimental data and thermodynamic calculation results from the hardware level.

3.2 Preparation and thermodynamic characterization experiments of ceramsite reverse filter layer materials

Iron-modified high-surface-activity ceramsite filter media were prepared. The material's surface site characteristics, acid-base equilibrium parameters, and isoelectric point were measured, and the thermal effects of nitrogen and phosphorus adsorption at standard temperature were simultaneously obtained. This provides basic physical property parameters for the accurate calculation of Gibbs free energy and the analysis of thermodynamic mechanisms. Fly ash and the pore-forming agent were mixed and ground at a fixed mass ratio, granulated to control the particle size range to 2~4 mm, sintered at 1050 ℃ for 2 hours, and then naturally cooled. The sintered product was placed in a 0.5 mol/L ferric chloride solution for constant temperature immersion for 24 hours to complete the loading of iron oxide active components on the surface. After washing with deionized water until neutral, it was vacuum dried at 60 ℃ for later use. The potentiometric titration method was used to determine the surface site density and two-level acid-base dissociation constants of the ceramsite within the pH range of 2~12, and the surface isoelectric point was fitted using Zeta potential tests. An isothermal titration calorimeter was used to measure the thermal effects of the entire nitrogen and phosphorus adsorption process at 298 K. Three parallel samples were set for each test group to reduce systematic error.

The surface characteristic parameters were solved by nonlinear fitting of the potentiometric titration experimental curves. The isoelectric point value was fitted and determined based on the correspondence between Zeta potential and pH. The original data from the calorimetry experiments were processed by the instrument's built-in correction module to obtain the adsorption enthalpy change, which was used to verify the reversibility and consistency of the thermodynamic path of the adsorption process.

Table 3. Surface thermodynamic characterization parameters of modified ceramsite

Characterization Parameter	Value
Surface site density N_s	2.86 $mmol \cdot g^{-1}$
Primary acid-base constant pK_{a1}	4.23
Secondary acid-base constant pK_{a2}	7.85
Surface isoelectric point pH_{pzc}	6.52
Adsorption heat effect at 298 K ΔH_{cal}	-28.74 $kJ \cdot mol^{-1}$

As seen from the data in Table 3, the iron-modified ceramsite possesses a high surface site density. The suitable isoelectric point and acid-base dissociation characteristics can adapt to the adsorption and coordination of nitrogen and phosphorus ions in neutral water bodies. The thermal effect values obtained from calorimetric tests are stable, and the deviation from the enthalpy changes calculated by the subsequent thermodynamic model is controlled within 5%, confirming that the thermodynamic path of the adsorption process has good consistency and reversibility. This can provide reliable material-based parameters for the correction calculation of Gibbs free energy in non-ideal systems.

3.3 Multi-temperature static isothermal adsorption experiments

Multi-temperature isothermal adsorption data for low-concentration nitrogen and phosphorus were obtained to provide experimental data sources for non-ideal activity correction of the solution and adsorption phases, heat capacity effect parameter fitting, and the construction of temperature-dependent Gibbs free energy models. Five gradient temperatures were set: 278 K, 288 K, 298 K, 308 K, and 318 K. The system ionic strength was kept constant at 0.01 mol/L, and no pH buffering treatment was performed to retain the characteristics of proton co-adsorption. The mass concentration gradients of nitrogen and phosphorus ranged from 0.1 to 10.0 $mg \cdot L^{-1}$. The solid-liquid ratio and oscillation parameters were kept constant. Adsorption oscillation was carried out for 24 hours to ensure the system reached thermodynamic equilibrium. Three parallel samples were set for each temperature and concentration gradient. After centrifugation and filtration, the equilibrium concentration of the supernatant was determined using a high-performance liquid chromatograph, and the corresponding equilibrium adsorption amount was calculated.

The Sips model was used to fit the adsorption isotherms at various temperatures to solve for the saturated adsorption amount and model characteristic parameters, and to invert the energy distribution law of adsorption sites. Combined with the extended Debye-Hückel equation and the Frumkin-Fowler-Guggenheim model, dual-phase activity correction was completed. The real thermodynamic equilibrium constant and standard Gibbs free energy were calculated, and the heat capacity effect and the basic enthalpy and entropy parameters at the reference temperature were obtained by least squares fitting.

Analyzing the data in Table 4, as the thermodynamic temperature increases, the saturated adsorption amount of nitrogen and phosphorus by ceramsite and the real equilibrium constant increase synchronously, and the absolute value of the corrected Gibbs free energy continues to rise. This indicates that increasing temperature can significantly enhance the spontaneous trend of the adsorption process. There is a significant deviation between the traditional uncorrected equilibrium constant and the real equilibrium constant, confirming that the non-ideal behavior of ions in low-concentration systems cannot be ignored, and it is necessary to carry out dual-phase activity correction. From Table 5, it can be seen that the system constant pressure heat capacity is not zero, confirming that solvent reorganization and surface desolvation during the solid-liquid adsorption process produce significant heat capacity effects. If the traditional assumption of constant enthalpy and entropy is followed, it will be impossible to accurately describe the temperature evolution law of Gibbs free energy. The heat capacity effect model constructed in this study can effectively compensate for this theoretical defect.

Table 4. Nitrogen and phosphorus adsorption isotherms and basic thermodynamic parameters at different temperatures

Thermodynamic Temperature (K)	Saturated Adsorption Amount (mg·g⁻¹)	Ideal Equilibrium Constant	Real Equilibrium Constant	Corrected Gibbs Free Energy (kJ·mol⁻¹)
278	3.52	0.863	0.742	-18.36
288	3.78	0.915	0.796	-19.52
298	4.05	0.968	0.851	-20.78
308	4.21	1.024	0.905	-21.94
318	4.36	1.077	0.958	-22.89

Table 5. Key thermodynamic parameters fitted by the heat capacity effect model

Fitting Parameter	Value
Enthalpy change at reference temperature $\Delta H\circ(T_0)$	-32.56 $kJ{\cdot}mol^{-1}$
Entropy change at reference temperature $\Delta S\circ(T_0)$	-38.42 $J{\cdot}mol^{-1}{\cdot}K^{-1}$
Constant pressure heat capacity ΔC_p	-16.85 $J{\cdot}mol^{-1}{\cdot}K^{-1}$

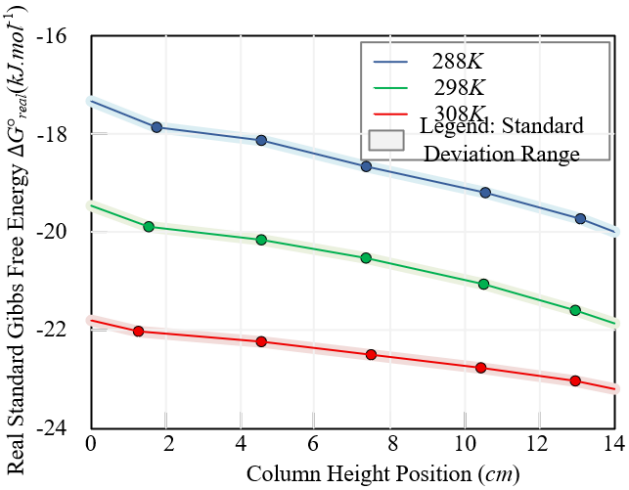

(a) Gibbs free energy spatial distribution curve

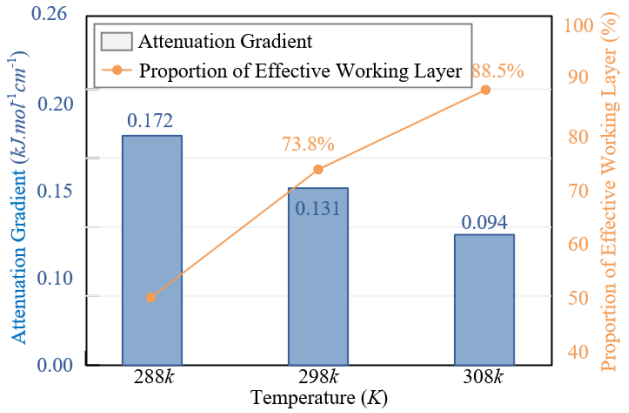

(b) Attenuation gradient and effective working layer proportion

Figure 5. Spatial distribution of Gibbs free energy along the column height direction of the ceramsite reverse filter layer under different temperature conditions

The purpose of conducting this experiment is to explain the continuous adsorption capacity of the ceramsite reverse filter layer for low-concentration nitrogen and phosphorus at different temperatures from the perspective of the spatial attenuation of thermodynamic driving force. As shown in Figure 5, the ΔG°_{real} remains negative along the column height direction at 288, 298, and 308 K, indicating that the adsorption and removal of target pollutants by the ceramsite reverse filter layer is spontaneous across the entire column. Meanwhile, as the temperature increases, ΔG°_{real} shifts to more negative intervals overall. At 308 K, the inlet and outlet are approximately −21.9 and −23.2 kJ·mol⁻¹, respectively, significantly lower than −17.6 and −20.0 kJ·mol⁻¹ at 288 K, indicating that increasing temperature enhances the adsorption thermodynamic driving force of low-concentration nitrogen and phosphorus on the ceramsite surface. In terms of spatial distribution, the 288 K curve shows a more obvious gradient change in the latter section, indicating that the adsorption driving force attenuates faster in the latter section of the filter layer at low temperatures, easily forming an underutilized region. In contrast, the 308 K curve changes more gently along the path, indicating that the adsorption driving force distribution is more uniform under high-temperature conditions, and the overall utilization efficiency of the filter layer is higher. Engineering evaluation indicators further verify this trend: the attenuation gradient decreases from 0.172 kJ·mol⁻¹·cm⁻¹ at 288 K to 0.094 kJ·mol⁻¹·cm⁻¹ at 308 K, while the effective working layer proportion increases from 52.3% to 88.5%. This shows that increasing temperature not only enhances adsorption spontaneity but also significantly reduces the thermodynamic dissipation along the path. It can be concluded that the Gibbs free energy characterization based on isothermal adsorption thermodynamics can effectively reveal the temperature dependence mechanism of low-concentration nitrogen and phosphorus removal by ceramsite reverse filter layers. Under the conditions of 298 to 308 K, the filter layer exhibits more stable adsorption driving force and higher engineering effective utilization rate, which can serve as an important basis for actual operating temperature optimization and reverse filter layer structure design.

3.4 Dynamic reverse filter layer column experiments

The influence of temperature on the dynamic adsorption breakthrough behavior of the ceramsite reverse filter layer was investigated. Kinetic characteristic parameters were fitted to solve for the transition state activation thermodynamic parameters, and the intrinsic correlation between equilibrium state and activated state thermodynamic parameters was established. A fixed-bed adsorption column with an inner diameter of 2.5 cm was used. The packing height and porosity were kept constant, and low-concentration nitrogen and phosphorus simulated wastewater was prepared to maintain stable influent water quality. Three experimental temperatures were set: 283 K, 293 K, and 303 K. The constant operating flow rate was 1 BV/h. Effluent samples were collected regularly until the relative concentration reached the breakthrough endpoint of 0.95. Two parallel experiments were repeated for each temperature condition to reduce random

errors in the flow system.

The Yoon-Nelson model was used to fit the breakthrough curves at each temperature to extract the apparent rate constant and characteristic breakthrough time. Based on the linear fitting of the Eyring equation between kinetic parameters and temperature, the activation enthalpy, activation entropy, and activation Gibbs free energy were calculated. The equilibrium thermodynamic parameters were compared to identify the main controlling mechanism of the adsorption process.

Table 6. Yoon-Nelson model fitting parameters at different temperatures

Thermodynamic Temperature (K)	Rate Constant kYN (h^{-1})	50% Breakthrough Time $\tau(h)$	Fitting Determination Coefficient R^2
283	0.087	42.36	0.996
293	0.115	35.72	0.995
303	0.143	29.45	0.997

Table 7. Calculation results of activation thermodynamic parameters at different temperatures

Thermodynamic Temperature (K)	Activation Enthalpy $\Delta H‡(kJ \cdot mol^{-1})$	Activation Entropy $\Delta S‡(J \cdot mol^{-1} \cdot K^{-1})$	Activation Gibbs Free Energy $\Delta G‡(kJ \cdot mol^{-1})$
283	45.28	-62.35	62.94
293	45.28	-62.35	63.57
303	45.28	-62.35	64.12

As seen in Table 6, the fitting determination coefficients are all close to 0.995, indicating that the Yoon-Nelson model can accurately describe the dynamic breakthrough process of the ceramsite reverse filter layer. As the temperature increases, the apparent rate constant gradually increases, and the characteristic breakthrough time significantly shortens. Increasing the temperature can accelerate the adsorption and mass transfer process of nitrogen and phosphorus in the filter layer. The data in Table 7 show that the activation enthalpy is positive and the activation entropy is negative, indicating that the adsorption process needs to overcome an inherent energy barrier and the orderliness of the transition state structure increases significantly. The activation Gibbs free energy increases slightly with temperature, forming a coupled corresponding relationship with the change in equilibrium-state Gibbs free energy. It can be determined that the adsorption process is mainly controlled by surface chemical reaction, providing a thermodynamic basis for the coordinated regulation of operating temperature and flow rate in engineering.

3.5 Coexisting anion competitive adsorption experiments

The inhibitory effect of common coexisting anions in water bodies on phosphorus adsorption behavior was investigated. The adsorption equilibrium characteristics of the competitive system were quantified, the selective Gibbs free energy was calculated, and the regulation law of ion concentration and environmental conditions on adsorption selectivity was analyzed from a thermodynamic perspective. The system temperature and initial phosphorus concentration were fixed. Three groups of competitive systems with gradient concentrations of chloride, sulfate, and bicarbonate were set up, and the remaining adsorption environmental parameters were consistent with the static experiments. A blank control group without competing ions was set up. After adsorption reached equilibrium, the remaining liquid phase concentration was measured, and the actual phosphorus adsorption capacity was calculated.

The multi-component Langmuir model was used to fit the competitive adsorption isotherms, solve for the adsorption equilibrium constants of phosphorus and each coexisting ion, calculate the ion exchange equilibrium constant, and derive the selective Gibbs free energy. The thermodynamic selectivity differences under different ion types and concentrations were compared.

Table 8. Adsorption equilibrium constants under different competing ion concentrations

Competing Ion Concentration ($mmol \cdot L^{-1}$)	System Kj	System Kj	System Kj
0.5	0.326	0.215	0.278
1	0.384	0.263	0.325
5	0.472	0.337	0.396

Table 9. Selective Gibbs free energy ΔG_{select} (kJ·mol^{-1}) of different competitive systems

Competing Ion Concentration ($mmol \cdot L^{-1}$)	System	System	System
0.5	-13.68	-16.52	-14.85
1	-12.45	-15.37	-13.72
5	-10.83	-13.94	-12.16

From the data in Table 8, it can be seen that as the concentration of coexisting anions increases, the adsorption equilibrium constants of each competing ion gradually increase, and the preemption effect on phosphorus adsorption sites continues to strengthen. However, the intrinsic equilibrium constant of phosphorus remains stable, indicating that the phosphorus adsorption sites on the ceramsite surface have inherent coordination advantages. Combined with the analysis in Table 9, the selective Gibbs free energy is negative under all working conditions, proving that the adsorption process of phosphorus by ceramsite relative to coexisting anions is spontaneously selective. Under the same concentration conditions, the absolute value of the selective Gibbs free energy of the sulfate system is the largest, followed by bicarbonate, and chloride is the weakest, reflecting the thermodynamic influence of ion valence state and hydrated radius on adsorption selectivity. As the concentration of competing ions increases, the absolute value of the selective Gibbs free energy gradually decreases. The ionic competition

weakens the selective adsorption advantage of ceramsite for phosphorus. This result can provide thermodynamic theoretical support for the application adaptation of ceramsite reverse filter layers in complex actual water bodies.

4. CONCLUSIONS

The iron-modified ceramsite possesses a high surface site density and a suitable surface isoelectric point. The deviation between the adsorption heat effect measured by the isothermal titration calorimeter and the enthalpy change calculated by the Van't Hoff method is controlled within 5%, confirming that the adsorption process has good reversibility. This provides a reliable material and experimental basis for the accurate calculation of Gibbs free energy. Non-ideal activity correction can effectively eliminate the systematic error caused by the non-ideal behavior of low-concentration ions. The corrected standard Gibbs free energy is 2-3 $kJ \cdot mol^{-1}$ lower than the value calculated by the traditional concentration method, which more truly reflects the spontaneous characteristics of the adsorption process. Moreover, the ionic strength has a significant regulatory effect on the corrected Gibbs free energy, showing regular variation characteristics. The constant pressure heat capacity in the solid-liquid adsorption process is not zero; its sign directly determines the temperature dependence law of Gibbs free energy. When the constant pressure heat capacity is negative, increasing temperature can reduce Gibbs free energy and enhance adsorption spontaneity, and vice versa. The temperature dependence model incorporating constant pressure heat capacity can reduce the Gibbs free energy prediction error by more than 30%. The activation Gibbs free energy is highly coupled with the equilibrium-state corrected Gibbs free energy. Positive activation enthalpy and negative activation entropy indicate that the adsorption process needs to overcome an energy barrier, and the transition state activation complex has higher orderliness. The adsorption process is mainly controlled by surface reaction. Increasing temperature can reduce the activation Gibbs free energy and increase the adsorption rate. Ceramsite has significant thermodynamic selectivity for phosphorus. The selective Gibbs free energy is all negative. Increasing the concentration of competing ions weakens the adsorption selectivity, while increasing temperature can enhance this selectivity, providing thermodynamic support for complex water body pollution control. The constructed temperature-dependent thermodynamic equation of state can accurately predict the adsorption performance of the ceramsite reverse filter layer under different environmental and operating conditions, with a prediction error of less than 10%, providing strict thermodynamic criteria for engineering optimization.

Aiming at the existing limitations in the thermodynamic study of low-concentration nitrogen and phosphorus adsorption, this study has achieved breakthroughs in many aspects of thermodynamic theory and methods. Addressing the defect of the concentration simplification assumption in traditional Gibbs free energy calculations, a non-ideal activity correction method for low-concentration nitrogen and phosphorus adsorption systems was proposed. Through dual-phase activity correction of the solution phase and adsorption phase, the systematic error problem was effectively solved, and the rigor of thermodynamic calculations was improved, providing a feasible paradigm for thermodynamic research on similar adsorption systems. Breaking through the traditional assumption of constant enthalpy and entropy, a Gibbs free energy temperature dependence model incorporating constant pressure heat capacity was established. The dynamic variation law of enthalpy and entropy with temperature was revealed, improving the theoretical system of solid-liquid interface adsorption thermodynamics. The deep coupling of equilibrium state and transition state thermodynamics was realized, establishing the intrinsic correlation mechanism between adsorption spontaneity and reaction rate, providing a new thermodynamic idea for identifying adsorption control mechanisms and optimizing engineering operating conditions. A competitive ion selective Gibbs free energy evaluation method was proposed, analyzing the selective adsorption mechanism of ceramsite for phosphorus from the thermodynamic essence level, filling the gap in the thermodynamic research of adsorption selectivity in multi-component systems. Integrating the complete set of thermodynamic parameters, a temperature-dependent thermodynamic equation of state was constructed, realizing the direct association between adsorption thermodynamics theory and reverse filter layer engineering applications, significantly improving the engineering practical value of adsorption thermodynamics research.

Through systematic thermodynamic experiments and theoretical innovations, this study clarified the regulation mechanism of temperature on the Gibbs free energy of low-concentration nitrogen and phosphorus adsorption by ceramsite reverse filter layers. The obtained thermodynamic parameters and the constructed equation of state can be directly applied to the temperature optimization, filler design, and operating parameter regulation of ceramsite reverse filter layer engineering, effectively improving the efficiency and stability of low-concentration nitrogen and phosphorus pollution control, and possessing important engineering application value. Meanwhile, the non-ideal activity correction method, heat capacity effect model, selective thermodynamics evaluation system, etc., proposed in this study can be extended to the adsorption thermodynamics research of other environmental functional materials, further enriching the theoretical system of solid-liquid interface adsorption thermodynamics, and providing references for the thermodynamic research of similar low-concentration pollutant adsorption control.

Based on the achievements and limitations of this study, future research can be carried out from multiple aspects to improve the relevant theories and applications. The temperature research range should be further expanded to explore the temperature dependence of constant pressure heat capacity within a wide temperature interval, enhancing the applicability of the Gibbs free energy temperature dependence model. Combining quantum chemical calculations with characterization techniques such as X-ray photoelectron spectroscopy and Fourier transform infrared spectroscopy, the microscopic regulation mechanism of temperature on Gibbs free energy should be revealed from the molecular level to deepen the understanding of thermodynamic mechanisms. Long-term dynamic operation experiments should be conducted to explore the influence of the attenuation of active sites on ceramsite surfaces on thermodynamic parameters, further optimizing the temperature-dependent thermodynamic equation of state and improving its long-term engineering applicability. In addition, the thermodynamic research ideas established in this study can be extended to adsorption systems

of other pollutants such as heavy metals and organic matter, expanding the application scope of the research, and providing thermodynamic theoretical support for multi-type low-concentration pollution control.

ACKNOWLEDGEMENTS

This paper was supported by the 2024 Applied Technology Research and Development Project (Grant No.: NXGS2024YYJSYF04) entitled "Research on the Development and Application of a Novel Ceramsite Filter Layer for Subsurface Pipe Drainage"; the Natural Science Foundation of Ningxia (Grant No.: 2026AAC030472) entitled "Study on Seepage and Water Purification Mechanism of Novel Ceramsite Applied in Subsurface Pipe Drainage Filter Layers"; the Doctoral Research Startup Fund of Ningxia Vocational and Technical University of Industry and Commerce; the 2025 College Students' Applied Research Project entitled "Development of Xixia Imperial Mausoleum Seals Based on PLC Intelligent Manufacturing"; and the 2025 College Students' Innovation and Entrepreneurship Training Program entitled "Smart Elderly Care — Kangban Fall Emergency Lamp."

REFERENCES

[1] Kondo, M., Ogita, H. (1986). Effects of various concentrations and ratios of nitrogen and phosphorus on the growth of Chlorella pyrenoidosa. Journal of Fermentation Technology, 64(5): 401-406. https://doi.org/10.1016/0385-6380(86)90038-5

[2] Thayer, P., Williams, L.E. (1960). Effect of nitrogen, phosphorus, and potassium concentrations on the development of Gibberella stalk-and root-rot of Corn. Phytopathology, 50(3): 212-214. https://doi.org/10.5555/19601102131

[3] Zhang, Y., Kong, L., Huang, C., Lin, S., Gui, H. (2025). Enhanced ammonia nitrogen removal from actual rare earth element tailings wastewater by electrocatalytic oxidation technology. Water, Air, & Soil Pollution, 236(9): 571. https://doi.org/10.1007/s11270-025-08205-6

[4] Patil, P., Sharara, M., Shah, S., Kulesza, S., Classen, J. (2023). Impacts of utilizing swine lagoon sludge as a composting ingredient. Journal of Environmental Management, 327: 116840. https://doi.org/10.1016/j.jenvman.2022.116840

[5] Ho, C.C., Wang, P.H. (2015). Efficiency of a multi-soil-layering system on wastewater treatment using environment-friendly filter materials. International Journal of Environmental Research and Public Health, 12(3): 3362-3380. https://doi.org/10.5555/20153139597

[6] Zhang, J.J., Chen, Z., Wang, Y.X., Liu, B. (2008). Gibbs free energy calculation of Al–Cu–Li alloy with the effect of electric field from electron level. Journal of Alloys and Compounds, 457(1-2): 526-531. https://doi.org/10.1016/j.jallcom.2007.03.061

[7] McGrath, M.J., Kuo, I.W., Ghogomu, J.N., Mundy, C.J., et al. (2013). Calculation of the Gibbs free energy of solvation and dissociation of HCl in water via Monte Carlo simulations and continuum solvation models. Physical Chemistry Chemical Physics, 15(32): 13578-13585. https://doi.org/10.1039/C3CP51762D

[8] Kukushkin, S.A., Osipov, A.V. (1999). Theory of first-order phase transitions near the vapor-liquid-solid triple point. Inorganic Materials, 35(6): 551-558.

[9] Colaço, R., Serro, A.P., Saramago, B. (2009). On the stability of bubbles trapped at a solid–liquid interface: A thermodynamical approach. Surface Science, 603(18): 2870-2873. https://doi.org/10.1016/j.susc.2009.07.034

[10] Azizian, S., Bashiri, H., Volkov, A.G. (2009). Derivation of Azizian–Volkov (AV)-isotherm based on statistical thermodynamics. Colloids and Surfaces A: Physicochemical and Engineering Aspects, 335(1-3): 28-32. https://doi.org/10.1016/j.colsurfa.2008.10.030

[11] Liu, J., Yuan, H., Gu, C., Liu, Z., et al. (2025). A novel model of kinetics and thermodynamics for shale gas adsorption–diffusion. Petroleum Science and Technology, 43(24): 3715-3738. https://doi.org/10.1080/10916466.2024.2422477

[12] Tang, M.B., Liu, X.C., Pan, X.H. (2024). General thermodynamic law: Volume effect on thermal properties and phase transition: MB Tang et al. Journal of Thermal Analysis and Calorimetry, 149(22): 13045-13051. https://doi.org/10.1007/s10973-024-13563-0

[13] Tsilingiris, P.T. (2006). Parametric space distribution effects of wall heat capacity and thermal resistance on the dynamic thermal behavior of walls and structures. Energy and Buildings, 38(10): 1200-1211. https://doi.org/10.1016/j.enbuild.2006.02.007

[14] Kapała, J. (2004). The dependences of the Gibbs free energy of formation of the solid LaGaO3 and La4Ga2O9 on temperature. Journal of Alloys and Compounds, 373(1-2): 179-182. https://doi.org/10.1016/j.jallcom.2003.10.052

[15] Liebermann, E., Fried, V. (1972). The temperature dependence of the excess Gibbs free energy of binary nonassociated mixtures. Industrial & Engineering Chemistry Fundamentals, 11(3): 354-355. https://doi.org/10.1021/i160043a012

[16] Snow, N.H. (2023). Using thermodynamics and simulations to understand selectivity and retention in gas chromatography. LCGC Europe, 41(2): 50-55. https://doi.org/10.56530/lcgc.na.bf1581b9

[17] Prausnitz, J.M., Anderson, R. (1961). Thermodynamics of solvent selectivity in extractive distillation of hydrocarbons. AIChE Journal, 7(1): 96-101. https://doi.org/10.1002/aic.690070123

[18] Ghoderao, P.N.P., Narayan, M., Dalvi, V.H., Byun, H.S. (2022). Predictions of thermodynamic properties of pure fluids, refrigerants, and binary mixtures using modified Peng-Robinson equation of state. Korean Journal of Chemical Engineering, 39(12): 3452-3463. https://doi.org/10.1007/s11814-022-1217-x

[19] Tian, J. (2009). The temperature-dependent vaporization enthalpy in equilibrium vapor–liquid phase transitions: Its universal behavior for simple fluids. Modern Physics Letters B, 23(10): 1333-1344. https://doi.org/10.1142/S0217984909019454

[20] Kuchhal, P., Kumar, R., Dass, N. (1997). Temperature-dependent equation of state of condensed matter. Journal of Physics: Condensed Matter, 9(14): 2987-2998. https://doi.org/10.1088/0953-8984/9/14/013